Hindawi Publishing Corporation
Science and Technology of Nuclear Installations
Volume 2012, Article ID 646327, 25 pages
doi:10.1155/2012/646327

Research Article

Preliminary Assessment of the Possible BWR Core/Vessel Damage States for Fukushima Daiichi Station Blackout Scenarios Using RELAP/SCDAPSIM

C. M. Allison,[1] J. K. Hohorst,[1] B. S. Allison,[1] D. Konjarek,[2] T. Bajs,[2] R. Pericas,[3] F. Reventos,[3] and R. Lopez[4]

[1] *Innovative Systems Software, 1242 South Woodruff Avenue, Idaho Falls, ID 83404, USA*
[2] *ENCONET, Miramarska 20, 10000 Zagreb, Croatia*
[3] *ETSEIB, Universitat Politècnica de Catalunya, Avenida Diagonal 647, 08028 Barcelona, Spain*
[4] *Comision Nacional de Seguridad Nuclear y Salvaguardias, Dr. Barragan 779, Cuarto piso, Colonia Vertiz Narvarte, Delegacion Benito Juarez, 03020 Ciudad de México, DF, Mexico*

Correspondence should be addressed to C. M. Allison, iss@srv.net

Received 11 January 2012; Accepted 6 March 2012

Academic Editor: Alejandro Nuñez-Carrera

Immediately after the accident at Fukushima Daiichi, Innovative Systems Software and other members of the international SCDAP Development and Training Program started an assessment of the possible core/vessel damage states of the Fukushima Daiichi Units 1–3. The assessment included a brief review of relevant severe accident experiments and a series of detailed calculations using RELAP/SCDAPSIM. The calculations used a detailed RELAP/SCDAPSIM model of the Laguna Verde BWR vessel and related reactor cooling systems. The Laguna Verde models were provided by the Comision Nacional de Seguridad Nuclear y Salvaguardias, the Mexican nuclear regulatory authority. The initial assessment was originally presented to the International Atomic Energy Agency on March 21 to support their emergency response team and later to our Japanese members to support their Fukushima Daiichi specific analysis and model development.

1. Introduction

Immediately after the accident at Fukushima Daiichi, Innovative Systems Software (ISS) and other members of the international SCDAP Development and Training Program (SDTP) [1, 2] started an assessment of the possible core/vessel damage states of the Fukushima Daiichi Units 1–3. The assessment included a brief review of relevant severe accident experiments and a series of detailed calculations using RELAP/SCDAPSIM [3, 4] for a representative BWR vessel and related cooling systems.

As described briefly in Section 2, the experimental review presented to the IAEA emergency response team included representative highlights and phenomena identified from separate effects experiments BWR specific and other bundle experiments [5, 6], performed by the Karlsruhe Institute of Technology (KIT), and selected in-pile experiments [7, 8]. The KIT experiments were limited to peak temperatures less than 2600 K and thus covered the initial stages of core heat up and melting including the liquefaction and relocation of BWR control blades, structural material, and fuel rod cladding. The in-pile experiments reached higher peak temperatures and included the liquefaction of the fuel and other oxidized cladding materials and the formation of ceramic melts and blockages.

As described in Section 3, a combination of RELAP/SCDAPSIM/MOD3.4 and RELAP/SCDAPSIM/MOD3.5 was used to perform the detailed calculations. Both versions use publically available RELAP5/MOD3.2 and MOD3.3 thermal hydraulic models and correlations in combination with the detailed fuel behaviour and severe accident (SCDAP) models and correlations [9, 10]. The RELAP/SCDAPSIM code is designed to predict the behavior of reactor systems during normal and accident conditions including severe accidents

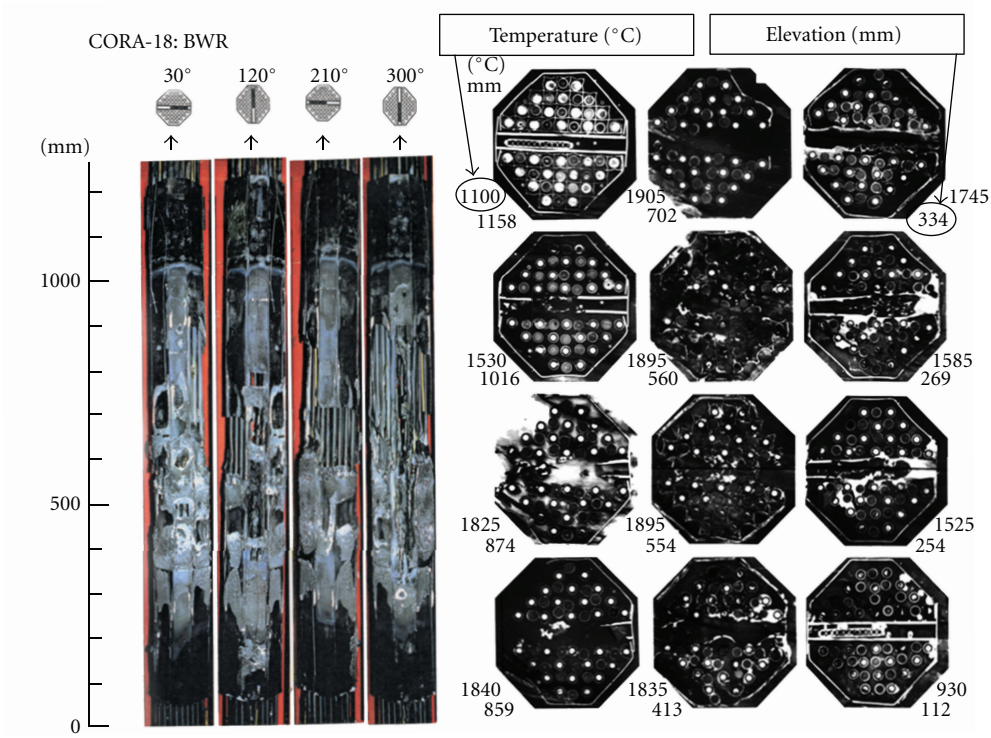

Figure 1: Posttest vertical view and horizontal metallographic cross-sections for CORA-18.

up to the point of reactor vessel failure. MOD3.4, the current production version, has been used by member organizations and licensed users to support a variety of applications including the design and analysis of severe accident experiments. MOD3.5, an experimental version of the code, has been used to support the design and analysis of the French PHEBUS-FP [11, 12], German QUENCH [13], and Russian PARAMETER [14] experiments and incorporates the latest SCDAP model improvements. It is the main version now being used by SDTP members and selected licensed users for Fukushima analysis and assessment.

As described in Section 4, the initial Laguna Verde RELAP/SCDAPSIM input models were provided by the Comision Nacional de Seguridad Nuclear y Salvaguardias (CNSNS), the Mexican nuclear regulatory authority. The Laguna Verde BWRs are BWR5 designs with thermal power of ~2370 MW and 444 fuel assemblies with an average core burnup of 3.57×10^5 MWs/Kg. For comparison, Fukushima Daiichi Unit 1 has a thermal power of 1380 MW from 400 assemblies. Units 2 and 3 have thermal powers of 2381 MW from 548 assemblies.

The initial RELAP/SCDAPSIM calculations performed prior to March 21st included a series of station blackout transients with a variety of emergency core cooling and depressurization strategies. Representative results are provided in Section 5. Additional calculations performed between March 21st and 25th to support the IAEA emergency response team included a variety of scenarios with loss of emergency core cooling ranging from 0 to 70 hours after scram. Representative results from these additional calculations are presented in Section 6.

As discussed in Section 7, these calculations which showed the core uncovery, fuel melting, and relocation of the fuel and other molten materials into the lower plenum can occur rather quickly once emergency cooling is no longer available. The timing of such events depends on the delays in the loss of emergency cooling as well as the specific details of an accident scenario such as the opening of safety relief valves to depressurize the vessel or the addition of water after partial or complete core uncovery.

The conclusions from the results and discussions presented in Sections 2, 3, 4, 5, 6 and 7 are presented in Section 8. This section first presents initial conclusions regarding possible core/vessel damage in Fukushima Daiichi Units 1–3. These initial conclusions are based on the information published and calculations performed in late March of 2011 immediately after the accident. Next, general conclusions for a typical BWR, Laguna Verde, subjected to "Fukushima-Daiichi-like" scenarios (short to extended periods of emergency core cooling after reactor scram, variation in vessel pressure, and water injection after core uncovery and start of core heat up) are presented. Finally the conclusions for severe accident management strategies are presented.

2. Highlights of Relevant Experiments and Phenomena

The existing data base and severe accident code and models developed over the past 40 years since the accident at TMI-2 are considered to be adequate to predict the likely states of a BWR core and vessel during "Fukushima-Daiichi-like"

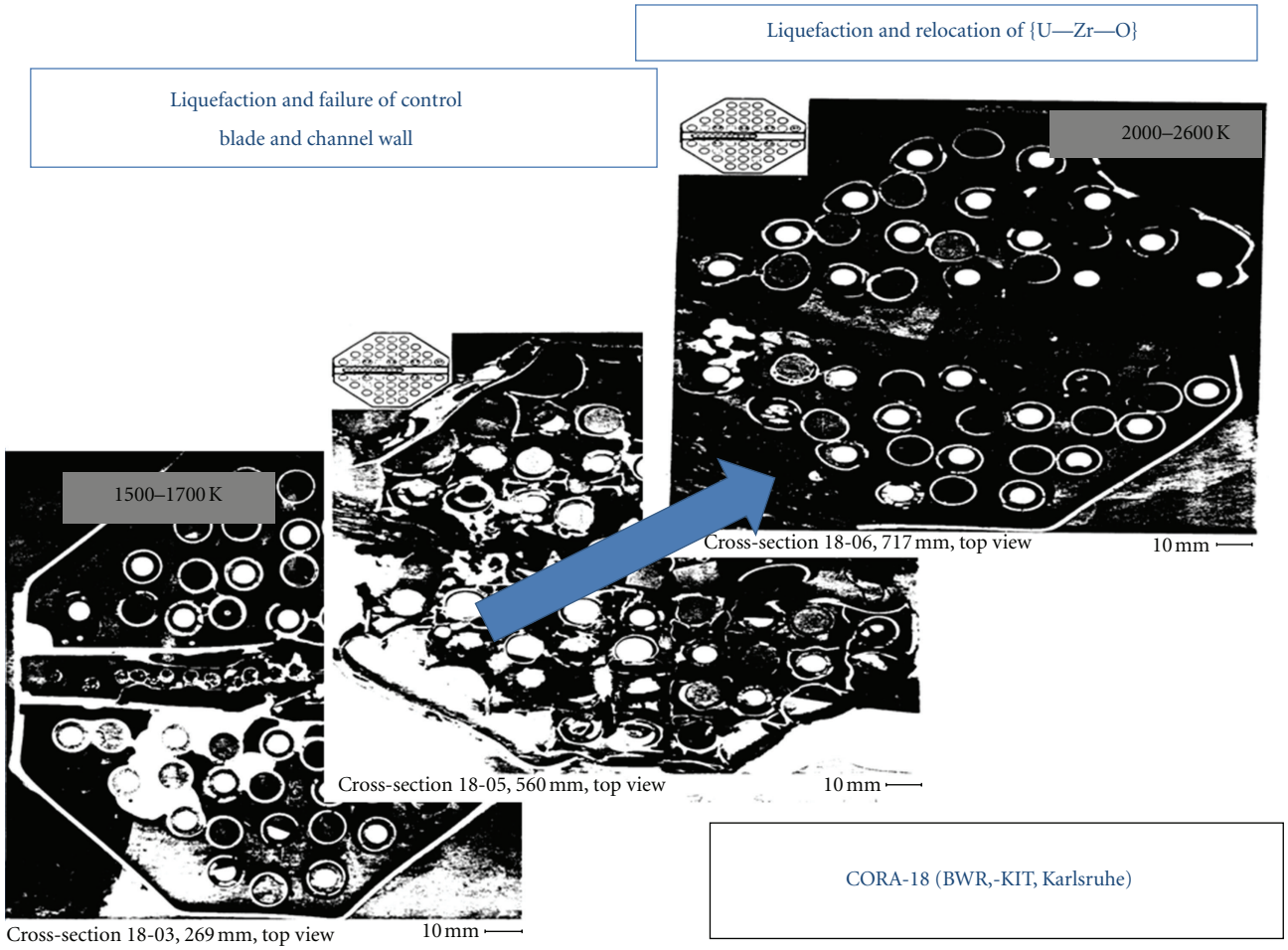

Figure 2: Horizontal metallographic cross-sections for CORA-18 showing destruction of control blade and channel box at temperatures between 1500–1700 K.

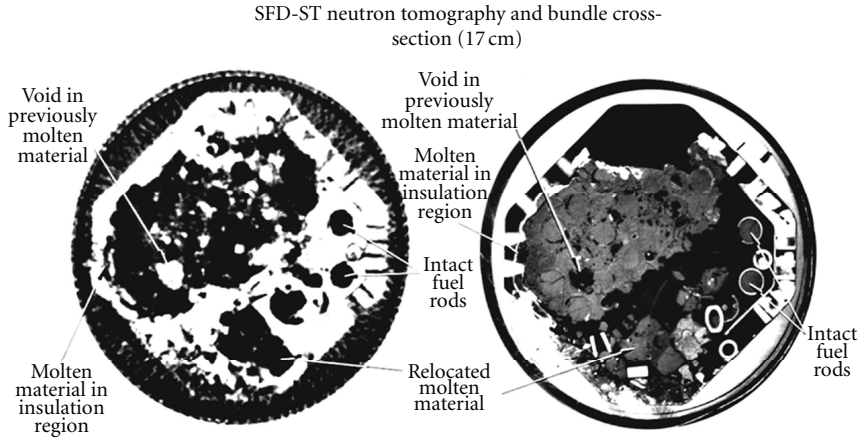

Figure 3: Horizontal metallographic cross-sections from PBF-SFD-ST showing blockage formation after {U-Zr}-O_2 melting and relocation.

scenarios. For Fukushima Daiichi Units 1–3, the dominant uncertainties in the predicted core/vessel states are associated with a lack of knowledge of actual operator actions as well as the possible damage to the reactor cooling systems caused by the earthquake. In particular, as noted in Section 7, operator actions to (a) activate or deactivate the emergency cooling systems, (b) depressurize the reactor vessel, and (c) initiate the addition of water to the vessel will have a significant impact on the heat up and melting of the core. Although it is likely that the analysis and final examination of the

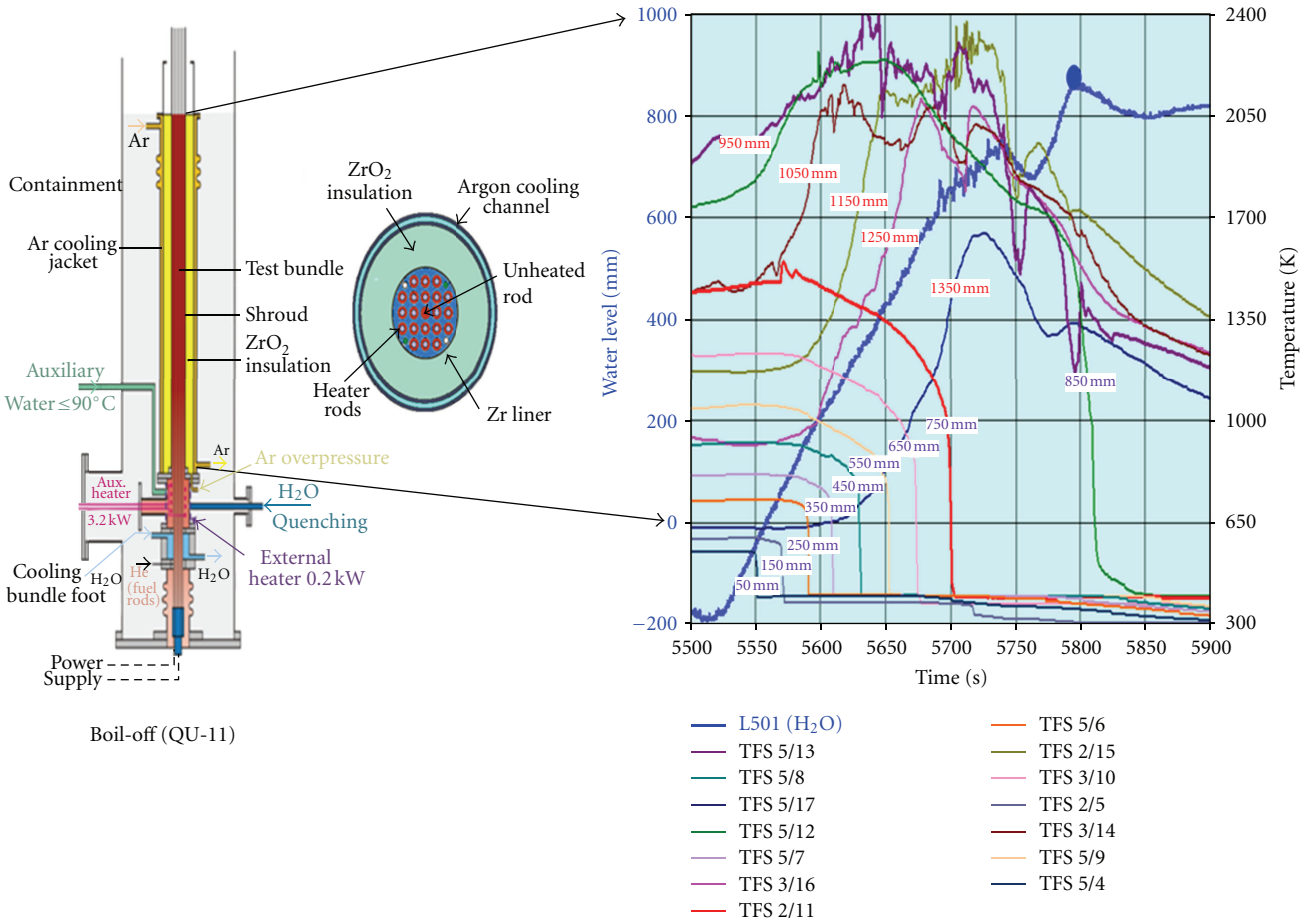

Figure 4: Measured temperatures and collapsed water level during the reflood phase in the Quench 11 experiment.

Fukushima Daiichi cores, vessels, and containments will identify gaps in our data base and models, it would be quite surprising if unexpected trends or phenomena are identified.

For now, it has to be concluded that the existing data base, including BWR specific bundle heating and quenching experiments, provides a good technical basis for the prediction of the progression of damage in a BWR core up to and including fuel melting or liquefaction ($T > 2800$ K). For example, Figures 1 and 2 show the progression of damage in a BWR bundle subjected to temperatures above 2200 K. These figures show metallographic cross-sections taken from the KIT CORA-18 experiment [15], a large BWR bundle subjected to a heat up to peak temperatures ranging from 1200 to 2200 K. The cross-sections of the more than 1 meter long bundle show the (a) liquefaction and failure of a control blade and channel wall (1500–1700 K), (b) liquefaction and relocation of {U—Zr—O} (2000–2200 K), and (c) formation of metallic blockages (1500–2200 K). At higher temperatures, since BWR specific materials and structures are destroyed at the lower temperatures, other in-pile experiments for PWR and BWR designs, as well as TMI-2, address the liquefaction and formation of {U-Zr}-O_2 molten pool(s) (2600–2800 K). For example, Figure 3 shows a metallographic cross-section at the upper part of the bundle where a previously molten mixture of {U-Zr}-O_2 had frozen for PBF-SFD-ST [16], a slowly heated (~0.5 K/s before the start of oxidation) fuel rod assembly of 914 mm.

The existing experiments also show clearly the impact of the addition of water once severe fuel damage has started. Experiments in the United States OECD LOFT-FP [8], German CORA and QUENCH, and Russian PARAMETER programs have shown the influence of water addition under a variety of conditions including flooding from the bottom, from the top, and flooding after the hot bundles have been exposed to air. For example, at heating rates typical of a station blackout with early loss of cooling, the addition of water can result in the accelerated oxidation of the Zircaloy cladding (and B_4C when present), significant increases in hydrogen generation, and the accelerated liquefaction and slumping of {U-Zr}-O_2. Figure 4 shows the results from one such experiment, the Quench 11 experiment [17], where the addition of water to the bottom of the assembly resulted in accelerated heating in the portions of the bundle where peak temperatures are above 1500 K.

3. RELAP/SCDAPSIM

RELAP/SCDAPSIM is designed to describe the overall reactor coolant system (RCS) thermal hydraulic response

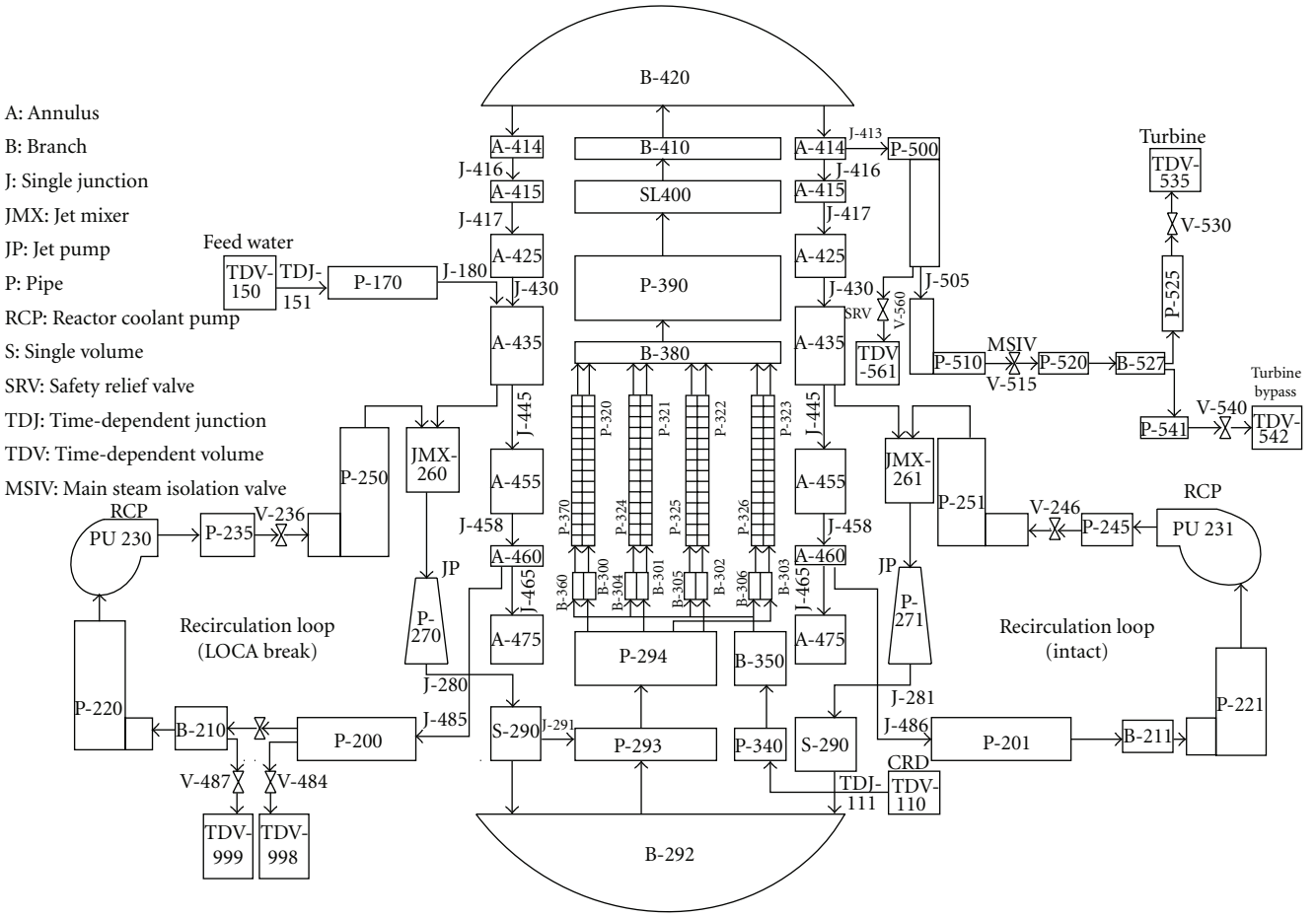

Figure 5: Overall Laguna Verde RELAP/SCDAPSIM thermal hydraulic component nodalization.

and core behaviour under normal operating conditions or under design basis or severe accident conditions. The RELAP5 models calculate the overall RCS thermal hydraulic response, control system behaviour, reactor kinetics, and the behaviour of special reactor system components such as valves and pumps. The SCDAP models calculate the behaviour of the core and vessel structures under normal and accident conditions. The SCDAP portion of the code includes user-selectable reactor component models for LWR fuel rods, Ag-In-Cd and B_4C control rods, BWR control blade/channel boxes, electrically heated fuel rod simulators, and general core and vessel structures. The SCDAP portion of the code also includes models to treat the later stages of a severe accident including debris and molten pool formation, debris/vessel interactions, and the structural failure (creep rupture) of vessel structures. The latter models are automatically invoked by the code as the damage in the core and vessel progresses.

RELAP/SCDAPSIM/MOD3.5 is the first release with the new QUENCH/PARAMETER-experiment-driven SCDAP modelling improvements. The new SCDAP modelling options include (a) an improved fuel rod gap conductance model, (b) improvements in the electrically heated fuel rod simulator model, (c) improvements in the shroud model, and (d) models to treat the influence of air ingression. The improved electrically heated fuel rod simulator model now includes the option to model tantalum heater elements in addition to the tungsten heater elements historically used in the QUENCH and other European bundle experiments. The improved shroud models include enhanced user options to simulate some of the unique features of experimental facilities including options to better simulate the influence of the thermal-mechanical failure of the experimental shrouds during high temperature and quenching conditions. The air ingression modelling options account for the changes in Zircaloy oxidation kinetics and uptake of nitrogen due to the presence of air.

4. Laguna Verde Input Model

The overall thermal hydraulic nodalization for the RELAP/SCDAPSIM model is presented in Figure 5. The plant model, developed by CNSNS, has a high level of detail. It represents the important features of the core, vessel, associated emergency cooling systems, and containment. The nodalization includes the reactor pressure vessel (RPV), Figure 6, the water (safety) injection components of the emergency core cooling system (see Figures 6 and 7) and main steam line(s) (see Figure 8).

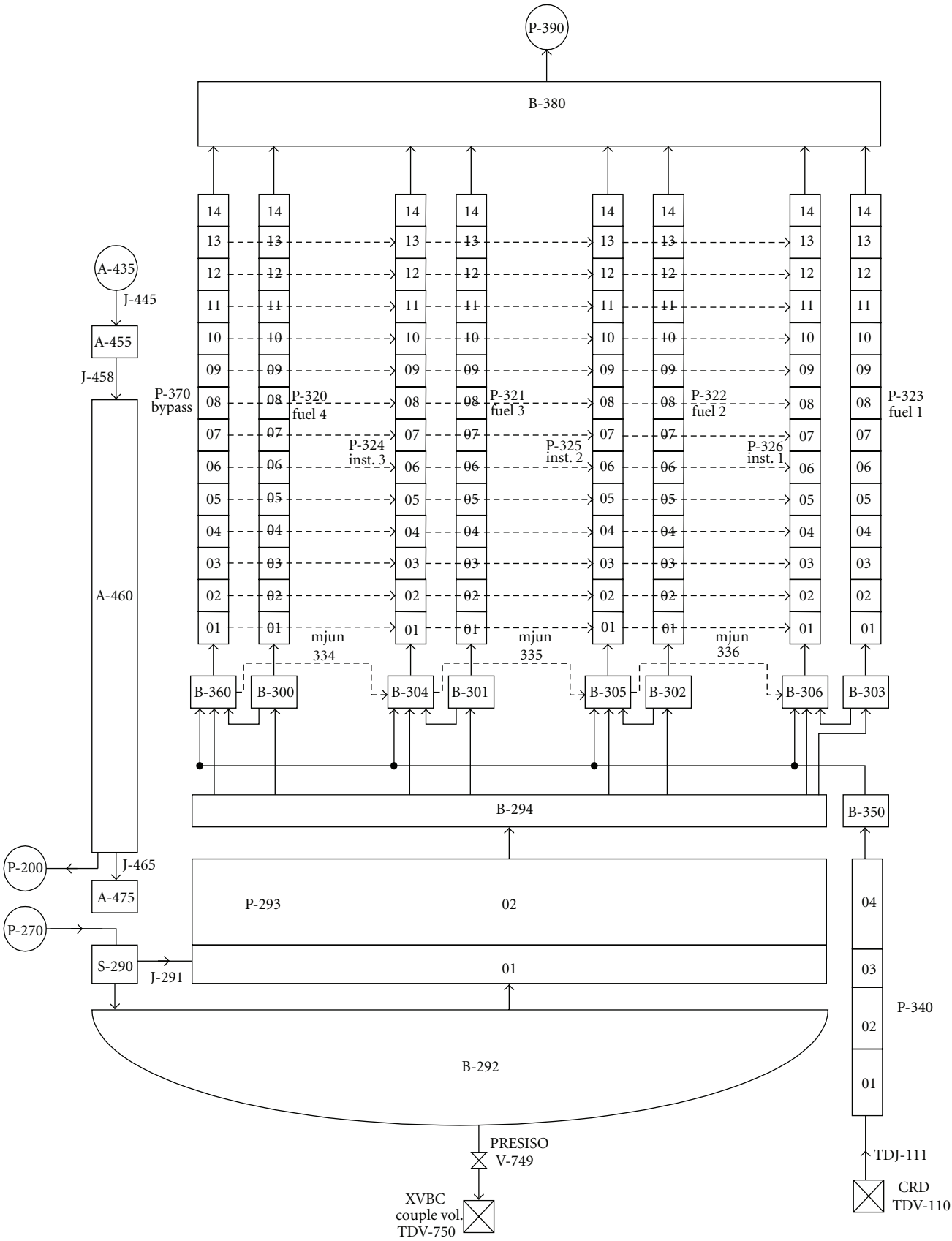

Figure 6: Laguna Verde: reactor pressure vessel and control rod drive (CRD) cooling system detailed nodalization.

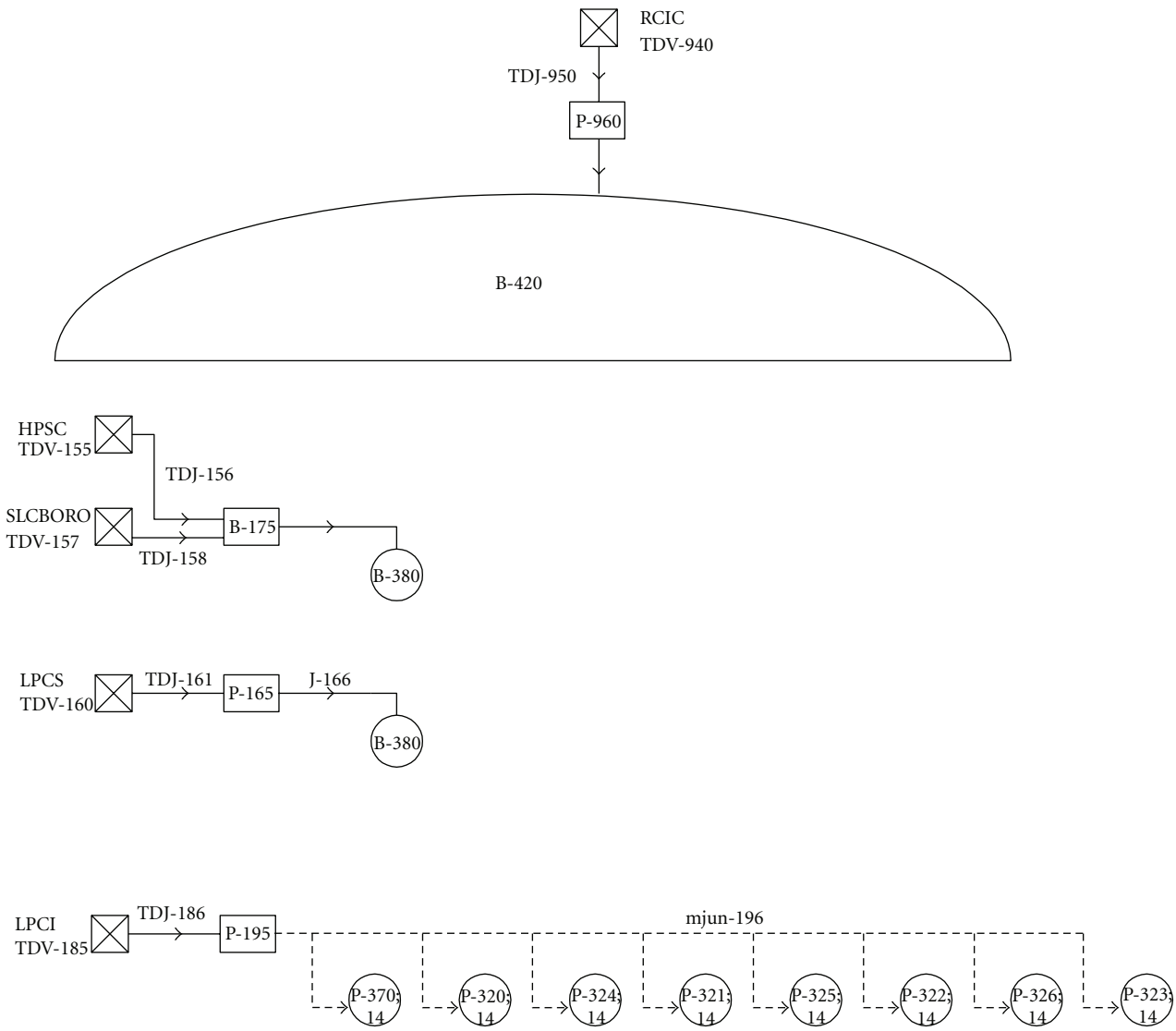

Figure 7: Laguna Verde: emergency cooling system water injection components.

Table 1: Timing of major damage progression events for a scenario with depressurization and termination of emergency water injection at 4.2 hours after reactor scram (CRD flows maintained).

Events	Time (s)	Time (hr)	Time after start of depressurization (hr)
Depressurization and termination of water injection in RPV	15000	4.2	
Initial fuel melting {U-Zr}-O_2	18000	5.0	0.8
Initial relocation of metallics (SS/Zr/B_4C) into LP	19500	5.4	1.3
Initial relocation of fuel {U-Zr}-O_2 into LP	20000	5.6	1.4

The core is described using four groups of representative BWR assemblies and associated control blade/channel boxes at different power levels and burnup histories (see Figure 6). Four vertical flow channels describe the flow within each of the four groups of BWR fuel assemblies (inside the fuel channels). An additional four vertical flow channels describe the flow in the bypass regions outside the channel boxes and surrounding the control blades. Each representative assembly in each group includes a representative fuel rod bundle, Zircaloy channel box, and B_4C control blade element, Figure 9. The fuel rods in each assembly are described by a representative SCDAP fuel rod component. The channel box and control blade segment in each assembly is described by a representative SCDAP BWR channel box/control blade component. The radial and axial power peaking for the four representative fuel rod groups are provided in Figure 10. The fuel rods in groups 1 and 2 (labelled components 1 and 2 in the figure) have average burnup levels of 4.34×10^5 MWs/kg.

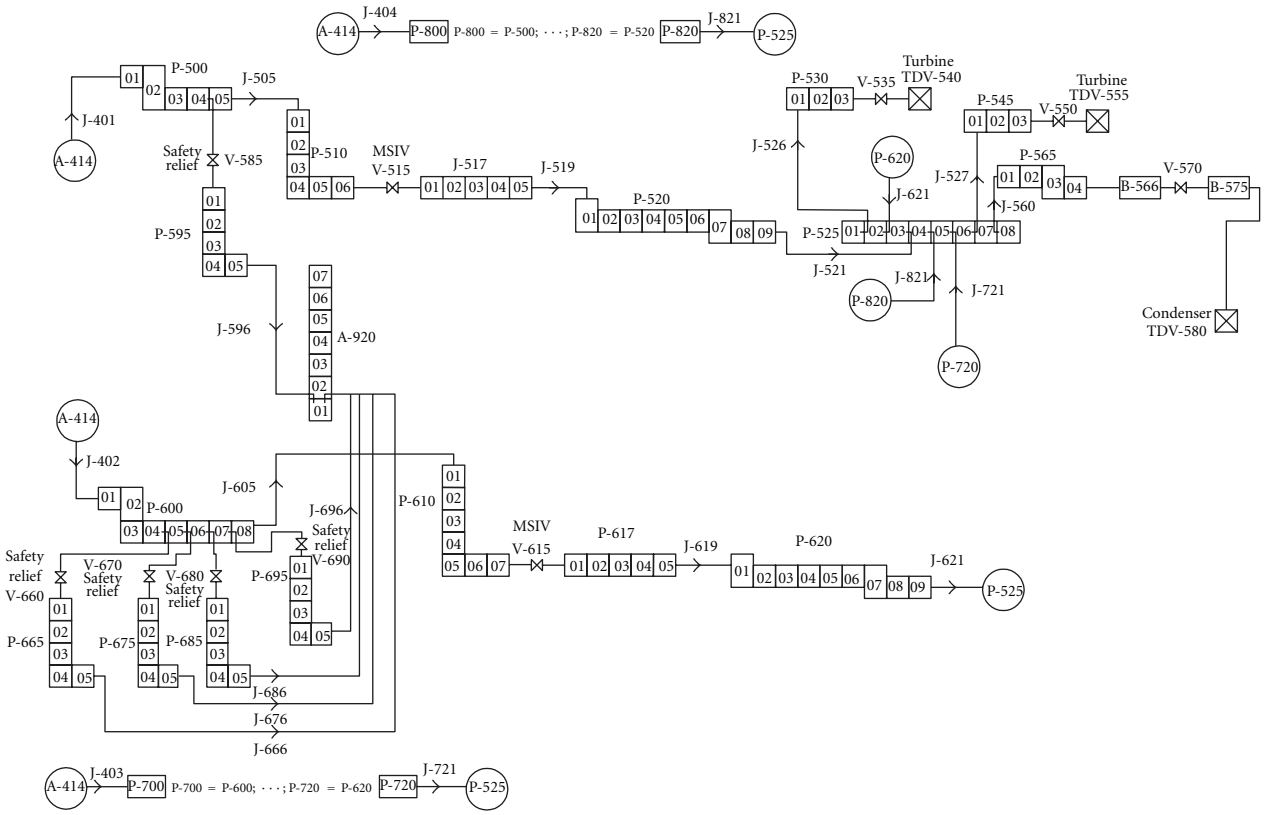

Figure 8: Laguna Verde: main steam line detailed nodalization.

Fuel rods in groups 3 and 4 have average burnup levels of 3.74×10^5 and 1.88×10^5 MWs/kg, respectively.

5. Initial Calculations in Support of IAEA Emergency Response Team (through March 24, 2011)

The initial calculations were performed by CNSNS using RELAP/SCDAPSIM for station blackout conditions with different scenarios after loss of emergency cooling including boil-off at high pressure and low pressure (opening of two safety relief valves (SRVs) after loss of emergency cooling). Additional calculations were then performed by ISS on March 21 to provide bounding results for the IAEA emergency response team. Since, at this time, it was not known what accident management strategies were possible or being performed, a series of calculations were initiated assuming that emergency water injection to the RPV was terminated, and only limited (2.33 kg/s) water injection to the core from the control rod drive (CRD) cooling system was continued for a range of times starting from 4 hours to 20 hours after reactor scram. The following results are from calculations where the reduction in emergency water injection was initiated ~4.2 hours after reactor scram. The reduction of water injection was initiated following the depressurization of the reactor by opening two SRVs. Table 1 shows the event timing in this case. Figure 11 shows the peak assembly temperatures, collapsed water level (relative to the bottom of the vessel), the growth of the {U-Zr}-O_2 molten pool in the core region (radius of a sphere of the same volume), and the height of the debris bed in the lower plenum. The water level shown is relative to the bottom of the lower plenum with the top of the fuel at ~9.0 m. Figures 12, 13, and 14 show the core temperature distributions at times between 5.0 to 5.6 hours after reactor scram. Figure 15 shows integral hydrogen production and collapsed water level. Figures 16, 17 and 18 show the lower plenum debris bed and lower head vessel wall temperatures after the relocation of molten {U-Zr}-O_2 into the lower plenum with detailed snapshots at 6.9 and 7.5 hours after scram.

Additional calculations were then performed from March 22 to 24 to determine the influence of delays in the reduction of emergency water injection (CRD flows were continued at 2.33 Kg/s). The results are shown below. Table 2 shows the comparison of event timing with depressurization and reduction in water injection starting periods ranging from ~4–20 hours after reactor scram. Figure 19 shows the water level and maximum core temperature for the different scenarios with the time referenced to the start of the depressurization. The water level shown is relative to the bottom of the lower plenum with the top of the fuel at ~9.0 m. Figure 20 shows the corresponding hydrogen generation.

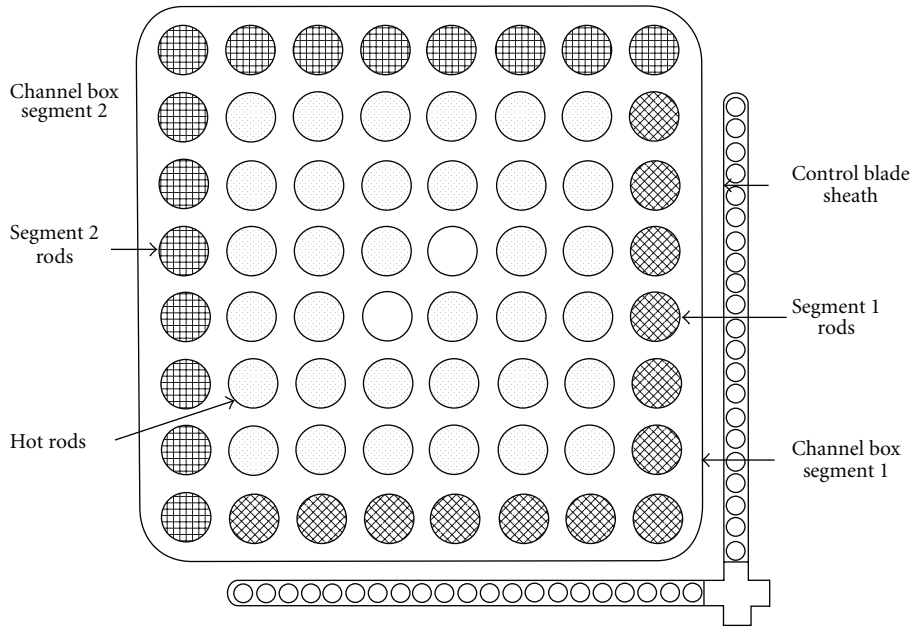

Figure 9: Representative RELAP/SCDAPSIM BWR assembly for Laguna Verde.

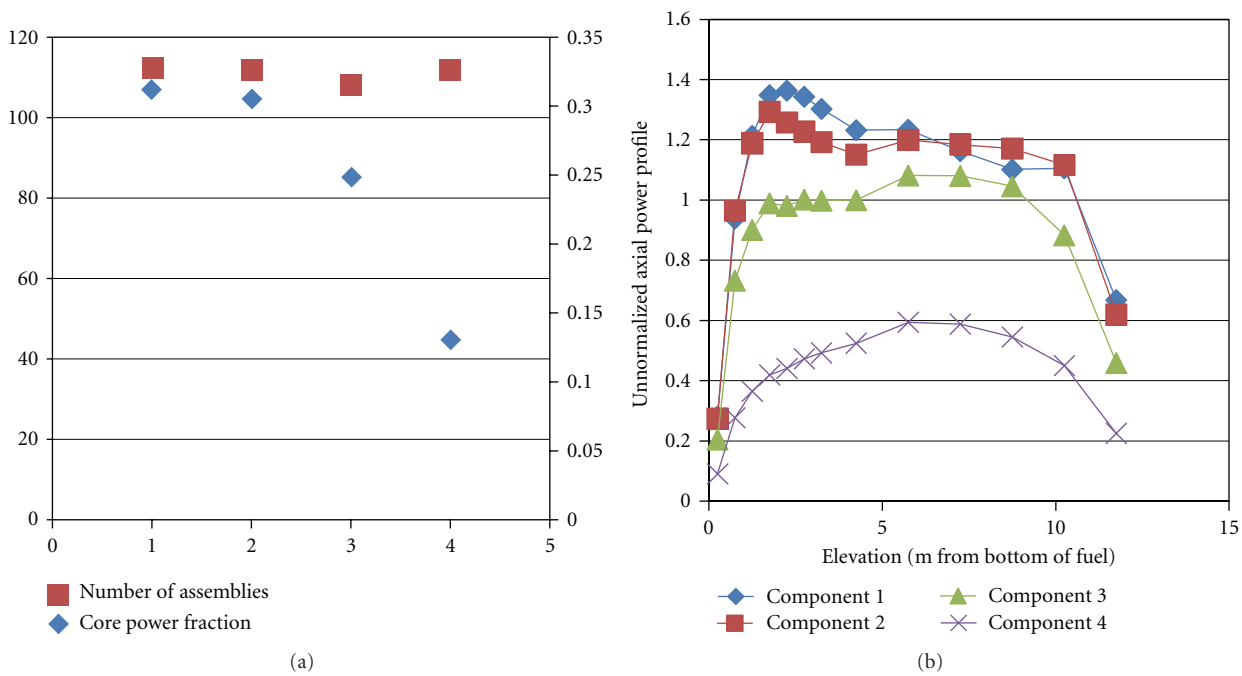

Figure 10: Description of the four representative assemblies used in the Laguna Verde input model.

6. Additional Calculations (March 25–April 24)

After March 25, additional calculations were initiated looking at a variety of different accident scenarios. These calculations included station blackout transients.

(1) Loss of cooling immediately after scram with depressurization and no emergency water injection.

(2) With different water addition scenarios with no or limited emergency cooling water starting 4.2 hours after scram including;

(a) Depressurization by opening 2 SRVs with variations in flow including the following;

(i) Termination of all water addition through emergency cooling systems.

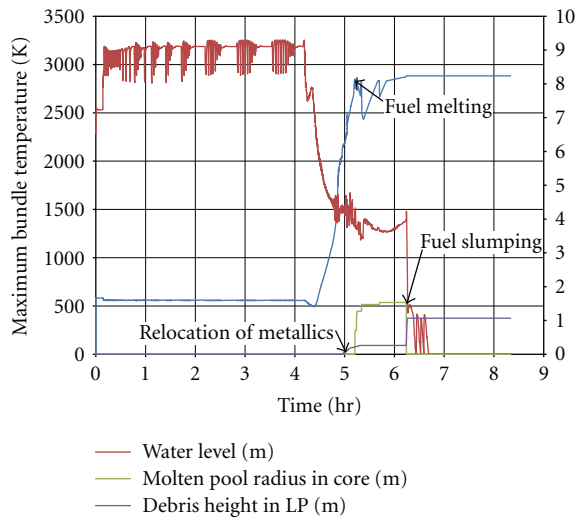

Figure 11: Maximum bundle temperature, water level, effective molten pool radius, and lower plenum debris height for a scenario with depressurization and termination of emergency water injection at 4.2 hours after reactor scram (CRD flows maintained).

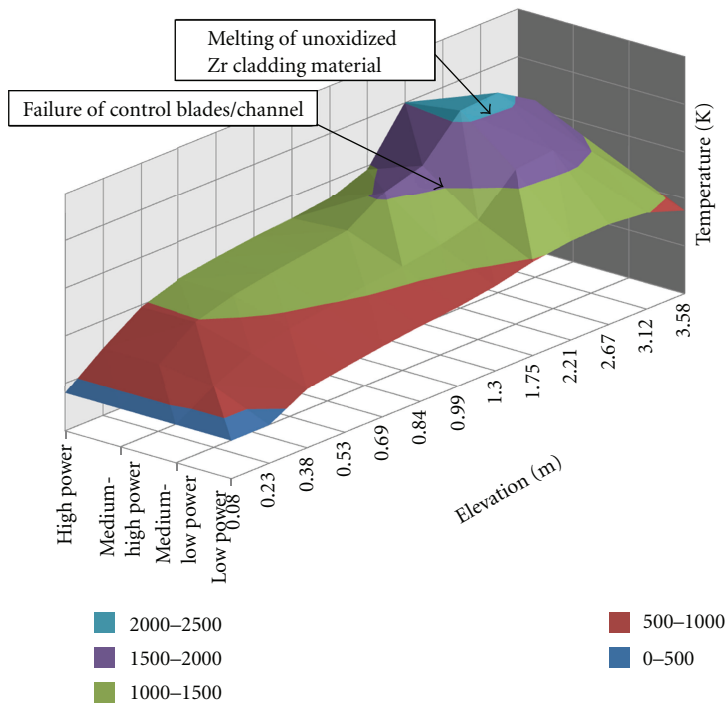

Figure 12: Core temperature distribution at 5.0 hours after reactor scram for a scenario with depressurization and termination of emergency water injection at 4.2 hours after reactor scram (CRD flows maintained).

(ii) Nominal CRD flows of 2.3 kg/s (base case from March 21st).
(iii) Doubled CRD flows of 4.6 kg/s.
(iv) Termination of all water addition for period of time followed by water injection at 4.7 and 5.3 hours after reactor scram.

(b) SRVs remained closed—high pressure varying between relief valve set points.

(3) With comparison of different scenarios initiated at 0, 4, 20, 40, and 70 hours after reactor scram.

As expected, the station blackout scenario immediately after scram resulted in the most rapid core uncovery, melting of the fuel, relocation of the fuel into the lower plenum, and likely lower head failure. In these calculations, the fuel in the reactor core was calculated to start liquefying at the time of 1.5 hours. By 2.2 hours, the molten pool extended to the periphery of the core. A molten pool

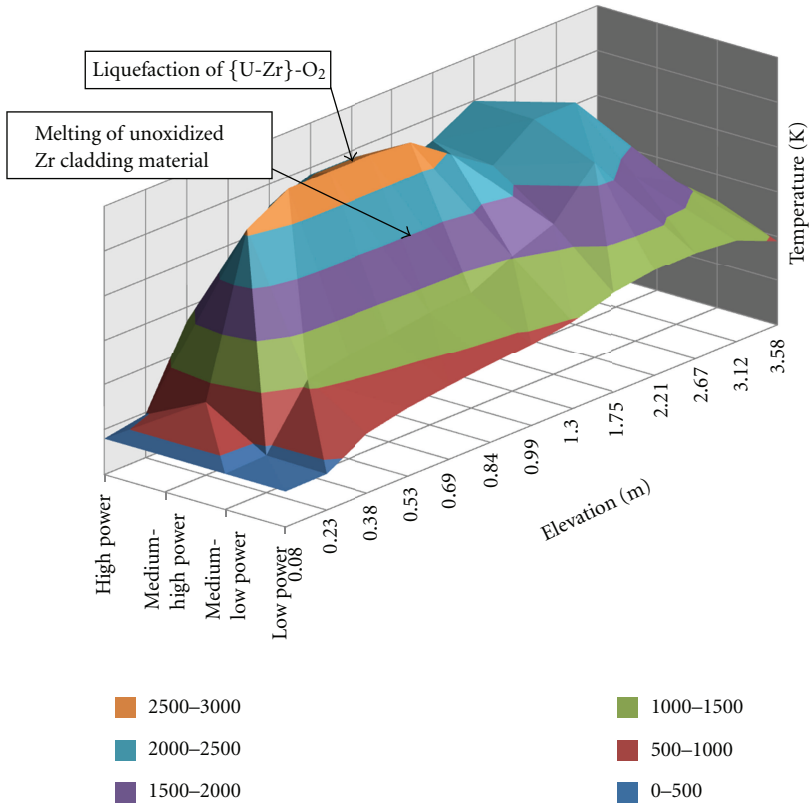

Figure 13: Core temperature distribution at 5.1 hours after reactor scram for a scenario with depressurization and termination of emergency water injection at 4.2 hours after reactor scram (CRD flows maintained).

containing 69,000 kg of liquefied {U-Zr}-O_2 was calculated to slump to the lower head at the time of 3.4 hours. At that time, the cumulative hydrogen production was 465 kg. The steam generated by the slumping caused another 150 kg of hydrogen to be produced in the next several hundred seconds. The maximum temperature in the lower head vessel wall had exceeded the melting point of steel within 4.3 hours.

The study of the influence of different water addition scenarios with no or limited emergency cooling water starting 4.2 hours after scram was a variation of the base calculations performed prior to and on March 21st. Figure 21 shows the influence of reactor vessel pressure on water level and maximum bundle temperature. In this case, the calculations considered a scenario where two safety relief valves (SRVs) were opened allowing the pressure to decrease to a value determined by the containment pressure versus a scenario where the SRVs were not opened and the vessel pressures were determined by the set points on the normal relief valves. Figure 22 shows the corresponding hydrogen generation rate and integral hydrogen production. Figures 23 and 24 show the influence of different scenarios of water injection once the core was starting to uncover. All of these scenarios maintained flow through the CRDs of 2.33 kg/s. Figure 23 shows the maximum bundle temperature, water level, and reactor vessel pressure. Figure 24 shows the corresponding hydrogen generation rate and integral hydrogen production.

The comparisons of different scenarios initiated at different times varying from 0 up to 70 hours after reactor scram included a significant variation in the decay heat levels at the time of core uncovery as well as variations in the reactor system pressure and water injection. The variation in decay heat for the Laguna Verde model is shown in Figure 25. Figure 26 shows the maximum bundle temperatures and water levels for high-pressure scenarios (SRVs remain closed) for scenarios where all of the emergency water injection was terminated at a time varying from 0 hours after scram to 70 hours after scram. Figure 27 shows the corresponding hydrogen production for these scenarios. Figures 28 and 29 show the influence of different scenarios at reduced decay heats with loss of emergency cooling at 40 and 70 hours. The scenarios start out similarly with a high-pressure scenario, but in the 70 hour scenario, the two SRVs were opened approximately 2 hours after the loss of emergency cooling.

7. Discussion of Results

The calculations for a wide range of station blackout scenarios showed that the core uncovery, fuel melting, and relocation of the fuel and other molten materials into the lower plenum can occur rather quickly once emergency cooling is no longer available. For the scenarios with the loss of emergency cooling occurring within 2 or 3 days after reactor scram followed by the opening of the SRVs and

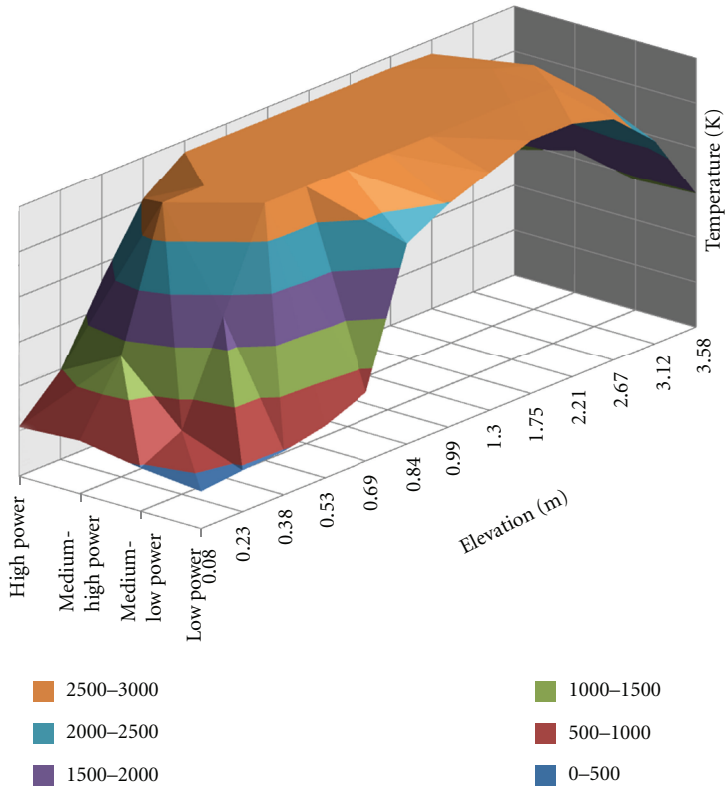

Figure 14: Core temperature distribution at 5.6 hours after reactor scram for a scenario with depressurization and termination of emergency water injection at 4.2 hours after reactor scram (CRD flows maintained).

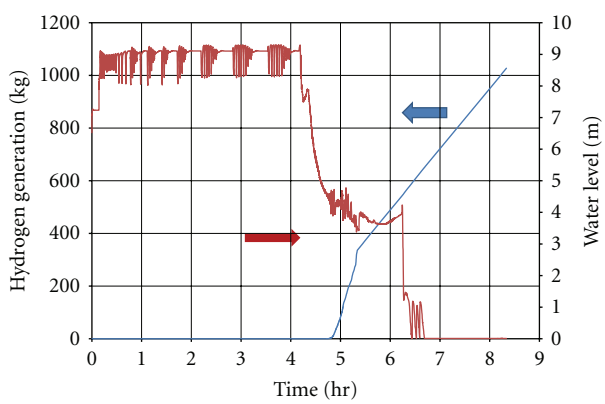

Figure 15: Hydrogen generation and water level for a scenario with depressurization and termination of emergency water injection at 4.2 hours after reactor scram (CRD flows maintained).

Table 2: Timing of initial fuel melting for scenarios with depressurization and termination of emergency water injection at 4.2, 11.8, and 19.6 hours after reactor scram (CRD flows maintained).

Depressurization and termination of water injection in RPV (hr)	Initial fuel melting {U-Zr}-O_2 Time after start of depressurization (hr)
4.2	0.8
11.8	1.5
19.6	1.9

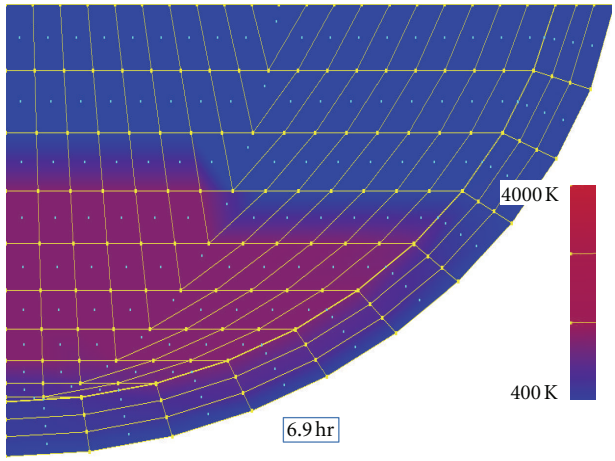

Figure 16: Temperatures in lower plenum at 6.9 hours for a scenario with depressurization and termination of emergency water injection at 4.2 hours after reactor scram (CRD flows maintained).

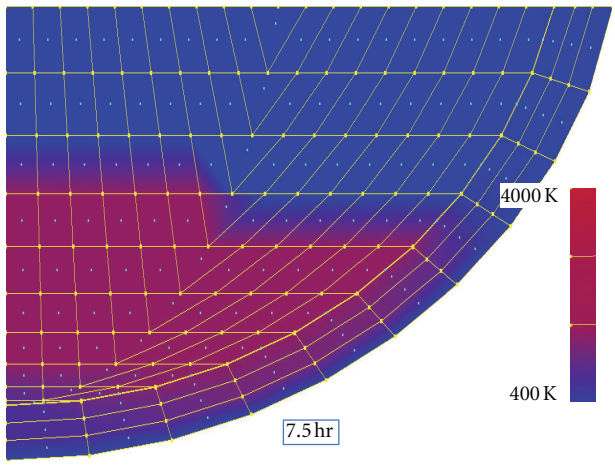

Figure 17: Temperatures in lower plenum at 7.5 hours for a scenario with depressurization and termination of emergency water injection at 4.2 hours after reactor scram (CRD flows maintained).

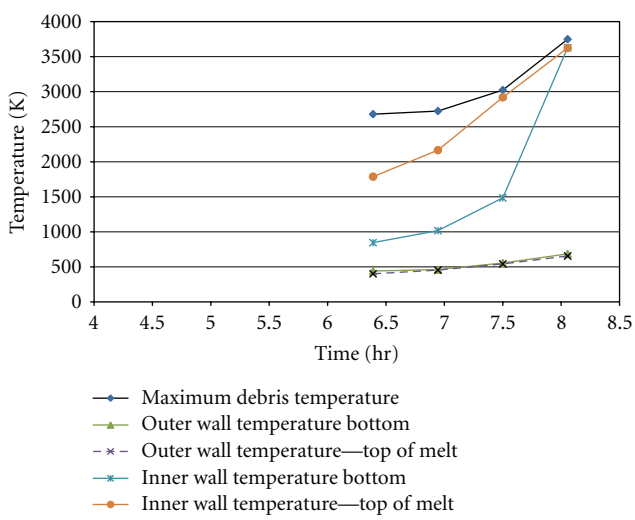

Figure 18: Temperatures in lower plenum wall and debris after melt relocation for a scenario with depressurization and termination of emergency water injection at 4.2 hours after reactor scram (CRD flows maintained).

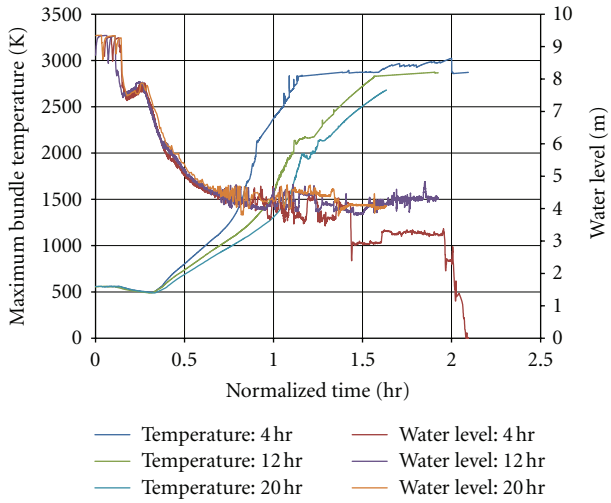

Figure 19: Maximum bundle temperature and water levels for scenarios with depressurization and termination of emergency water injection at 4.2, 11.8, and 19.6 hours after reactor scram (CRD flows maintained).

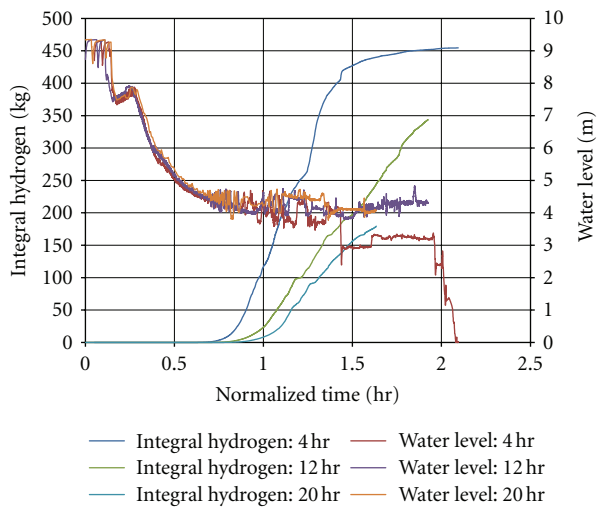

Figure 20: Integral hydrogen production and water levels for scenarios with depressurization and termination of emergency water injection at 4.2, 11.8, and 19.6 hours after reactor scram (CRD flows maintained).

depressurization, fuel melting can be reached within 2 hours of the loss of core cooling. For the same scenarios but keeping the SRVs closed (high-pressure scenarios), fuel melting can be delayed for some hours (approximately 2 hours for a scenario with loss of cooling about 4 hours after scram). This delay is more pronounced for scenarios with a loss of cooling after 2 or 3 days. See Table 2 and Figures 19, 21, and 26, for example.

Although the timing of core damage is impacted by the timing of the loss of emergency cooling, the pattern of the radial and axial extent of the damage in the core does not change significantly. This can be seen by comparing the temperature distributions in the core for the two scenarios where the vessel is depressurized in conjunction with loss of emergency cooling at 4.2 and 40 hours after scram, respectively. Figures 30 and 31 show the temperature distributions after failure of the control blades and channel boxes at temperatures near 1500 K and after the start of the melting of the unoxidized cladding material at temperatures near 2000 K in the hottest regions of the core. The pattern is quite similar even though the 4.2 hour scenario still has limited cooling with the injection of water through the CRD cooling system, while the 40 hour scenario has no water injection. The limited CRD flow in the 4.2 hour scenario results in the bottom of the core remaining relatively cool compared to the rest of the core.

The impact of the axial power distribution in the core is also apparent in the radial and axial extent of core damage. As identified in Figure 10, the axial power distribution for the high and medium-to-high power assemblies actually has a double axial power peak even though the bottom peak is much higher. In contrast, the medium-to-low and low-power assemblies have a cosine power profile with the peak near the center of the core height. The impact of the variation in the

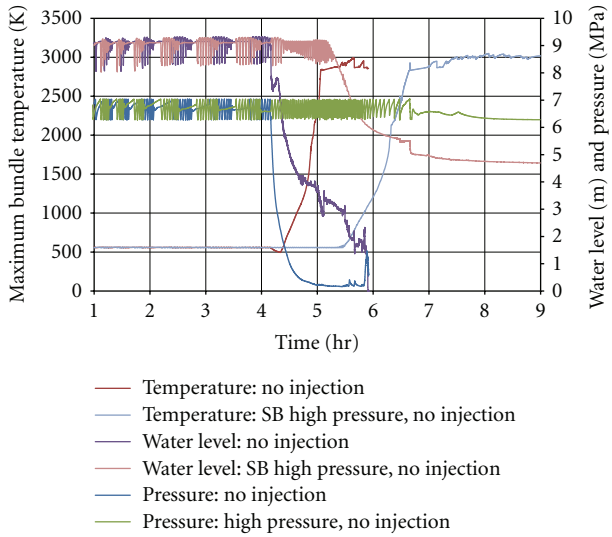

Figure 21: Maximum bundle temperature, water level, and reactor vessel pressure for scenarios with and without water injection after the start of core uncovery (all emergency water injection was terminated at 4.2 hours after reactor scram).

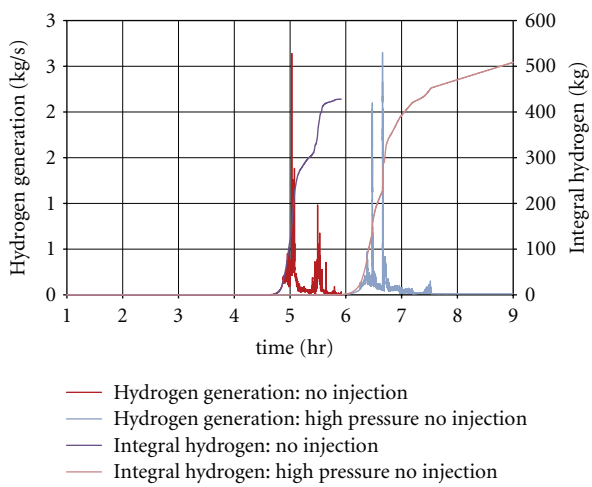

Figure 22: Hydrogen generation rate and integral hydrogen for scenarios with and without water injection after the start of core uncovery (all emergency water injection was terminated at 4.2 hours after reactor scram).

power profile from the high-to-low power assemblies shows up in the noticeable double hump in the temperatures for the higher-power assemblies visible in Figures 30 and 31.

The radial and axial extent of the damage in the core is much more impacted by the changes in thermal hydraulic conditions associated with the opening (or lack of opening) of the SRVs. Figures 32 and 33 show the core temperature distributions at differing times after the start of core uncovery for the scenarios where the emergency core cooling is terminated at 4.2 hours after reactor scram. Figure 32 shows the scenario where the SRVs are opened resulting in a depressurization of the vessel. Figure 33 shows the scenario where the SRVs are not opened, so the vessel pressure cycles between the normal relief valve set points but remains high through the scenario. As shown in Figure 21, the main contributor to the difference in the temperature distributions in these two scenarios is the much higher water level at the time of initial core heating and melting for the high-pressure scenario. That is why the higher temperatures and associated damage are limited to the upper portion of the core in the high-pressure scenario. A secondary factor, also identified in Figure 21, is that the cycling of the pressure due to the opening and closing of the normal relief valve impacts the oxidation in the core. That is, as the relief valve opens and the pressure drops, the steam generation rate and associated oxidation rate increase (in the higher temperature and higher elevation regions where oxidation is limited by the availability of steam).

The influence of water addition can be seen by comparing the results shown in Figures 34–38. Figure 34 shows the maximum core temperature, water level, and pressure for two scenarios where the emergency water cooling was terminated and the vessel was depressurized. The core uncovery and heat up was initiated by the termination of

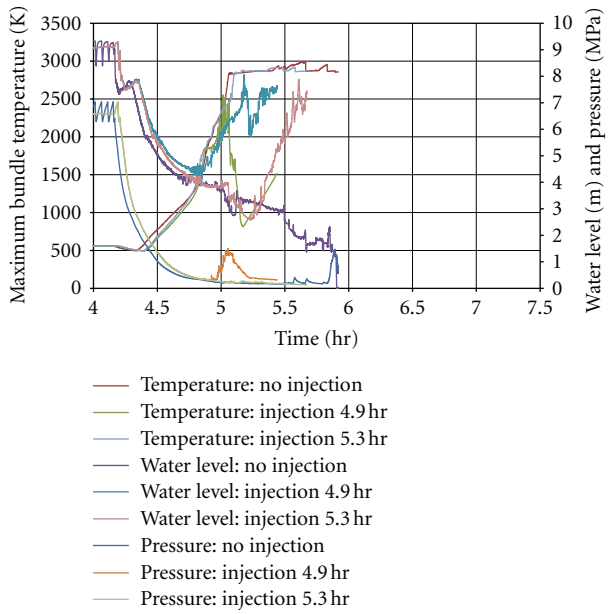

Figure 23: Maximum bundle temperature, water level, and reactor vessel pressure for scenarios with and without water injection after the start of core uncovery (all emergency water injection was terminated at 4.2 hours after reactor scram).

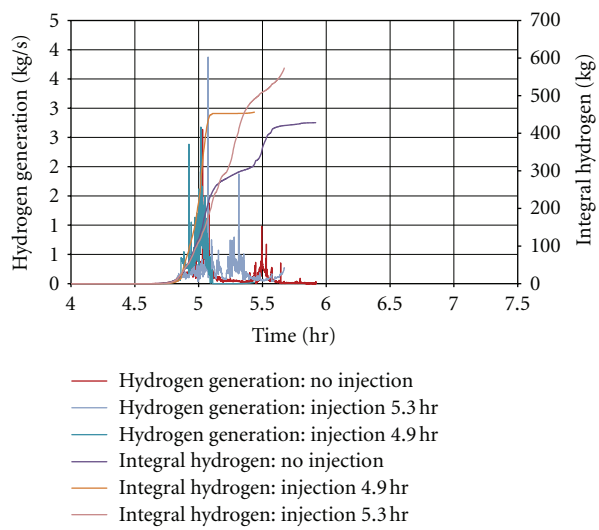

Figure 24: Hydrogen generation rate and integral hydrogen for scenarios with and without water injection after the start of core uncovery (all emergency water injection was terminated at 4.2 hours after reactor scram).

cooling and opening of two SRVs at 4.2 hours after scram. One of the scenarios allowed the core to continue to uncover, while the other scenario included the injection of water into the vessel starting at 4.7 hours after a portion of the core has reached temperatures in excess of 1500 K. Although water level in the core immediately started to increase at 4.9 hours in the scenario with water injection, the maximum core temperatures continue to climb to temperatures above 2500 K before starting to decrease. As shown in Figures 35–36, during the scenario with the water injection at 4.9 hours, the core temperatures also increased over more of the core initially and then reduced as water moved up into the core. Figure 35 shows the core temperature distribution at 5.0 hours after scram with temperatures in the high-power and medium-to-high power assemblies exceeding 1500 K (with the destruction of the control blades and channel boxes) over much of the assemblies above the water rising in the core. Figure 36 shows the core temperature at 5.1 hours after scram. Figure 37 compares the two scenarios with and without water injection at 4.9 hours at times of 5.0 and 5.1 hours after scram. The comparison at 5.0 hours after scram clearly shows that even though the peak core temperatures in the scenario with water injection was less than in the scenario without water injection, the extent of control blade and channel box melting and relocation is much larger in the case with water injection.

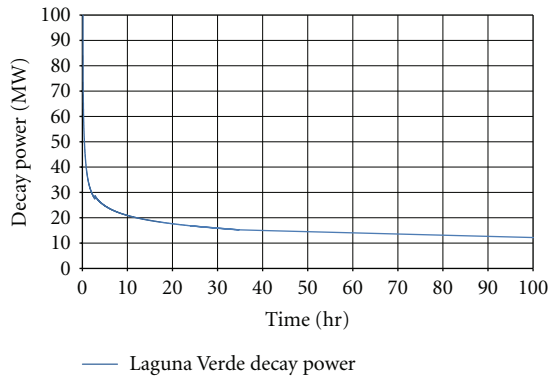

Figure 25: Variation in decay heat after reactor scram.

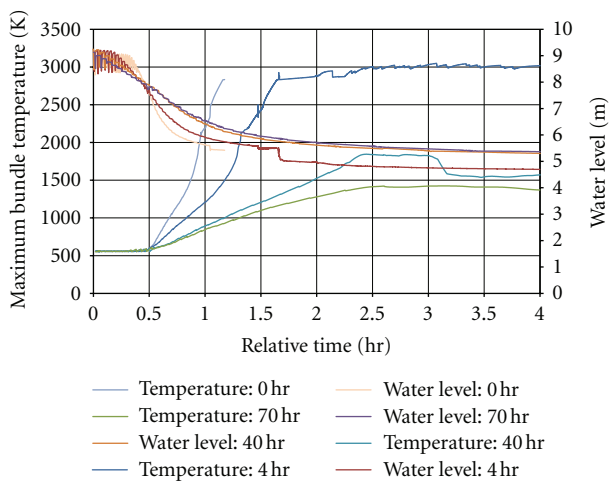

Figure 26: Maximum bundle temperature and water level for high-pressure scenarios for scenarios where all of the emergency water injection was terminated at a time varying from 0 hours to 70 hours after scram.

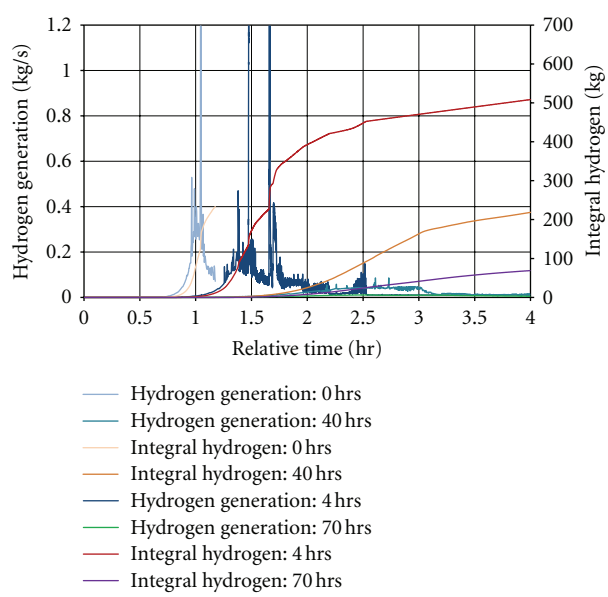

Figure 27: Hydrogen generation rate and integral hydrogen for high-pressure scenarios for scenarios where all of the emergency water injection was terminated at a time varying from 0 hours to 70 hours after scram.

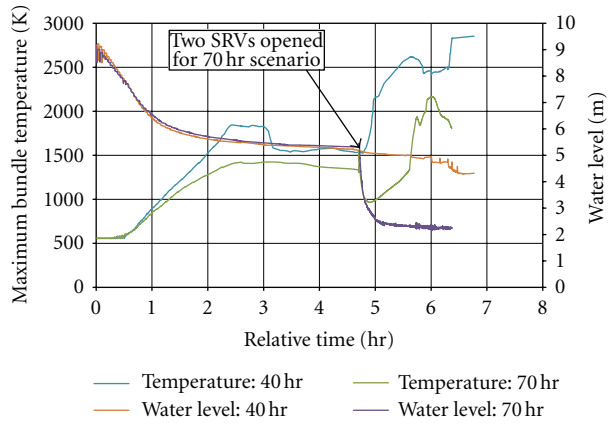

Figure 28: Maximum bundle temperature and water level for the two scenarios with initial loss of the emergency water injection at 40 hours and 70 hours.

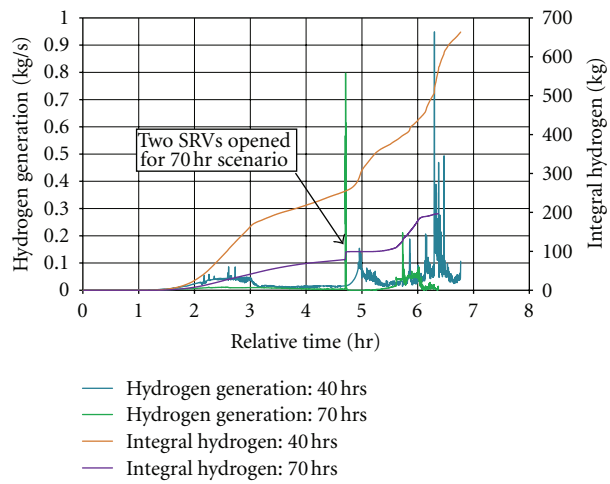

Figure 29: Hydrogen generation rate and integral hydrogen for the two scenarios with initial loss of the emergency water injection at 40 hours and 70 hours.

One of the important factors causing the greater extent of control blade/channel box destruction in the case with water injection can be seen in the results shown in Figure 38. In this figure, the hydrogen generation rate and integral hydrogen production are compared for the two scenarios with and without water injection at 4.9 hours. The comparison of the hydrogen generated in the two scenarios shows more hydrogen and associated oxidation heat generation over the period from 4.9 to 5.0 hours in the case with water injection. As discussed in Section 2, this type of behaviour was also clearly shown in the experiments with water addition like Quench 11.

8. Conclusions

The conclusions drawn from the preceding results and discussions are presented in three parts. First, what were the conclusions for the core/vessel damage expected in Units 1–3 of Fukushima Daiichi? These conclusions are based on the results and information reported for Fukushima in later March and early April, although the general information published to date appears to be consistent with the assessment presented in March to support the IAEA emergency response team and later to our Japanese colleagues. Second, what are general conclusions for a typical (Laguna Verde) BWR that may be subjected to Fukushima-Daiichi-like conditions? Third, what are the general conclusions for severe accident management strategies?

What were the conclusions for Units 1–3 of Fukushima Daiichi based on the assessment and information available in March?

(a) It was concluded within the first one or two weeks of the accident that it was likely that significant fuel melting occurred in Units 1 and 3 which lost cooling soon after loss of off-site power associated with the tsunami (Unit 1) and after approximately 40 hours (Unit 3), respectively.

(b) It was concluded that the failure of the vessel in Unit 1 was likely even given the large uncertainties in the accident conditions. Although it was considered

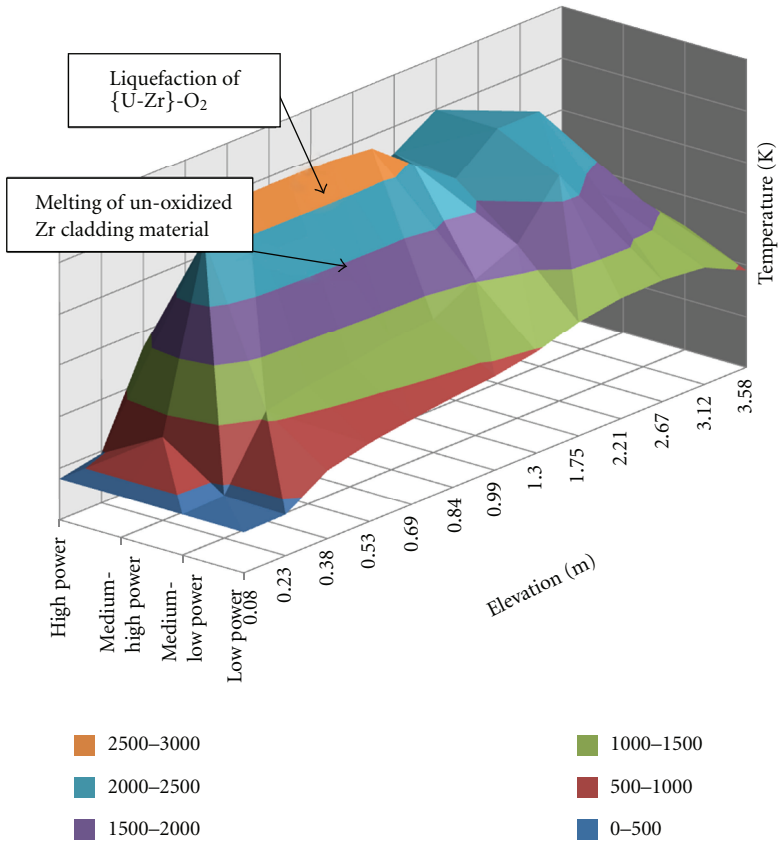

Figure 30: Core temperature at 5.1 hours for a scenario with depressurization (all emergency water injection excluding the CRDs was terminated at 4.2 hours after reactor scram).

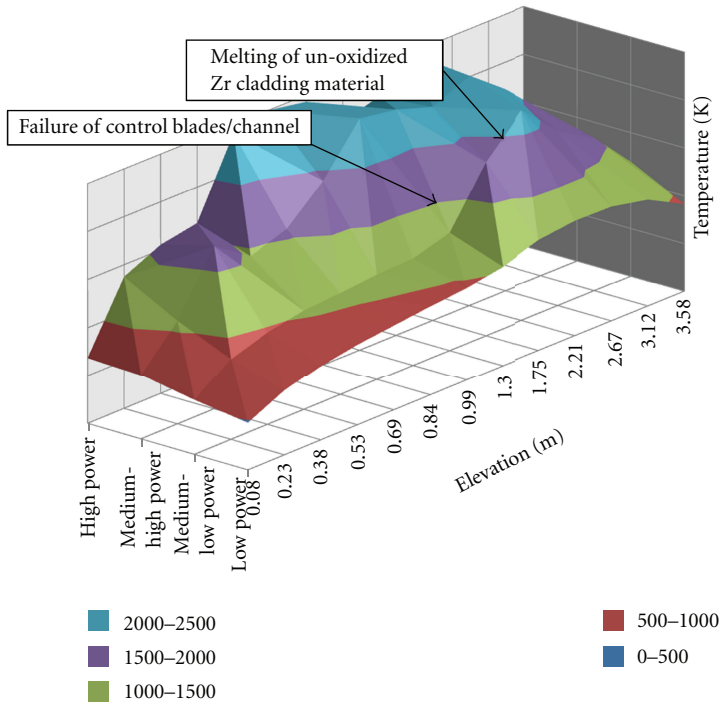

Figure 31: Core temperature at 41.7 hours for a scenario with depressurization (all emergency water injection was terminated at 40 hours after reactor scram).

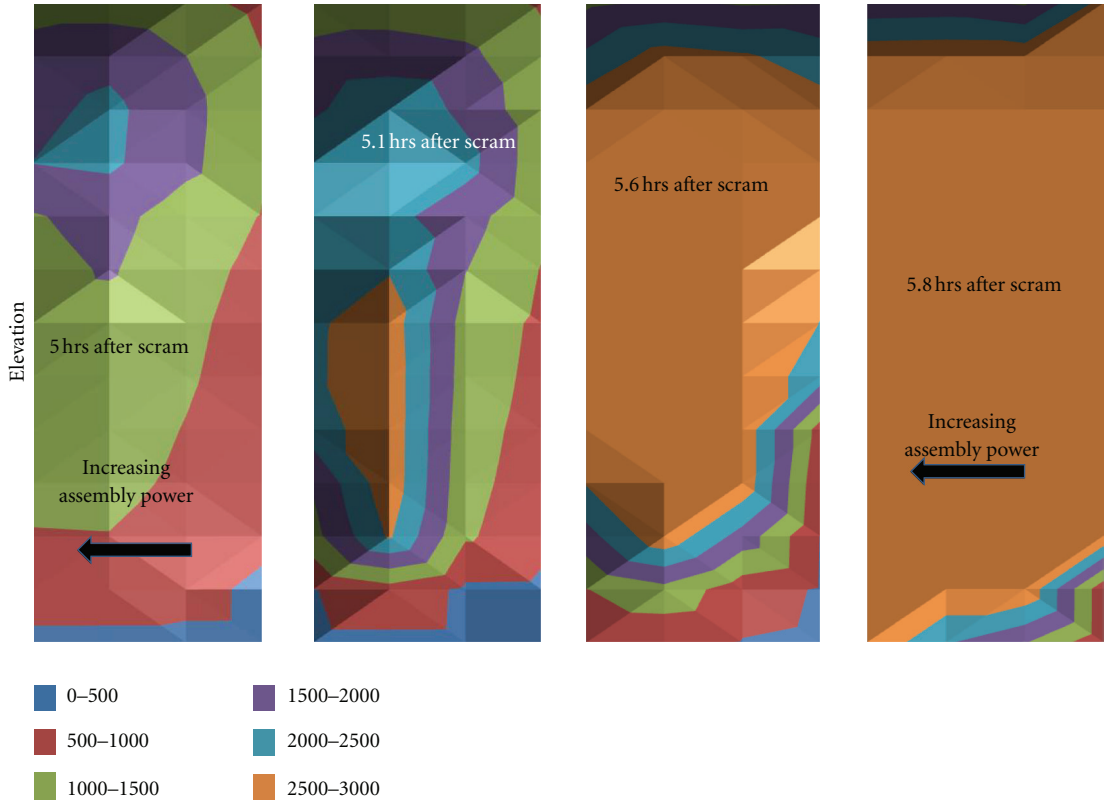

Figure 32: Core temperature distributions for a scenario with depressurization (all emergency water injection excluding the CRDs was terminated at 4.2 hours after reactor scram).

likely that the vessel in Unit 3 may have failed, the large uncertainties in the vessel pressure at the time that emergency cooling was lost precluded any definitive conclusions.

(c) It was concluded that some destruction of the core (in particular the loss of control blades and channel boxes) was likely in Unit 2, although the uncertainties associated with the attempts to depressurize the vessel at the same time salt water was being injected ruled out any definitive conclusions about fuel melting.

What are the general conclusions for a typical (Laguna Verde) BWR that may be subjected to Fukushima-Daiichi-like conditions?

(a) It only takes a few hours without emergency cooling for the core to uncover and the fuel to start melting. The time required to fuel melting temperatures will increase the longer that the emergency cooling can be maintained. In the calculations performed for Laguna Verde, the destruction of the control blades and channel boxes occurred within a few hours of loss of cooling even for scenarios with the emergency cooling maintained for three days (70 hours.) Thus, scenarios where cooling is maintained for a long period of time can result in a significant portion of the core without control blade material even though the fuel remains relatively intact.

(b) Intentional depressurization of the vessel after loss of cooling can have a very significant (negative) influence on the destruction and melting of the core. For the calculations for Laguna Verde, the depressurization of the vessel upon loss of emergency cooling accelerated the uncovery of the core and melting of the fuel to a significant degree. For the case of the loss of core cooling at 4 hours, the depressurization resulted in fuel melting within less than 1 hour, while in the high-pressure scenario under the same conditions, the fuel melting occurred more than an hour later. The fraction of the core reaching fuel melting temperatures also was increased by nearly a factor of two in the depressurization case at 4 hours. For scenarios with extended periods before emergency cooling is lost, the difference between depressurized and high-pressure scenarios becomes even more pronounced.

(c) The addition of water after the core is uncovered, and core temperatures which have exceeded 1500 K can have a mixed influence (positive and negative) on the destruction and melting of the core. The addition of water is necessary to slow or prevent the melting of the fuel but can result in the acceleration of the damage in the core initially, particularly the destruction of the control blades and channel boxes.

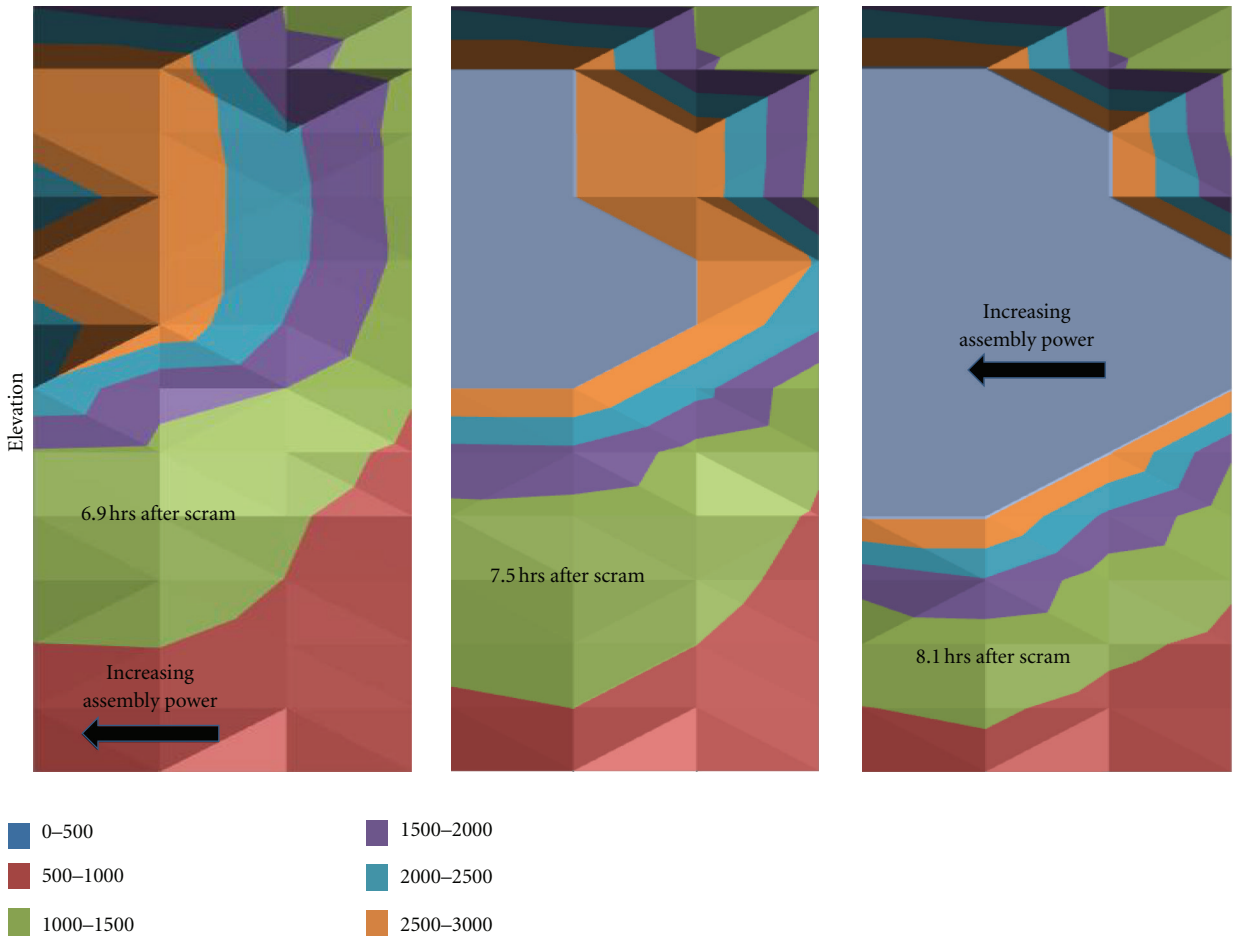

Figure 33: Core temperature distributions for a scenario without depressurization (all emergency water injection was terminated at 4.2 hours after reactor scram).

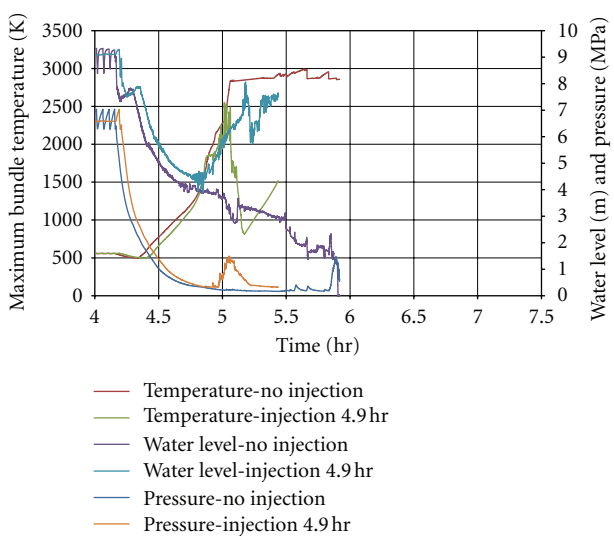

Figure 34: Maximum bundle temperature, water level, and reactor vessel pressure for scenarios without water injection and with water injection at 4.9 hours after scram (all emergency water injection was terminated at 4.2 hours after reactor scram).

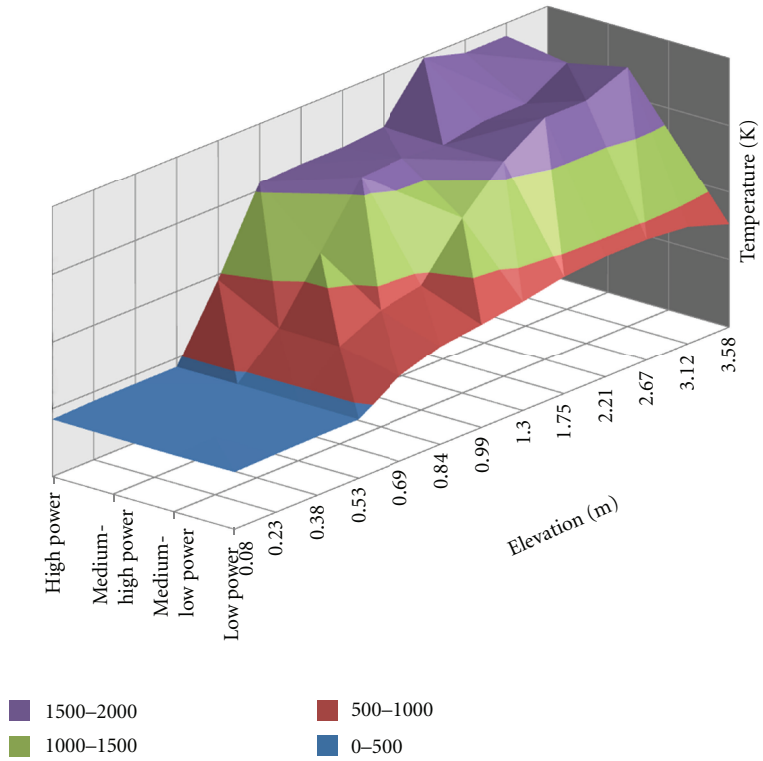

Figure 35: Core temperature distribution at 5.0 hours for scenario with water injection at 4.9 hours after scram (all emergency water injection was terminated at 4.2 hours after reactor scram).

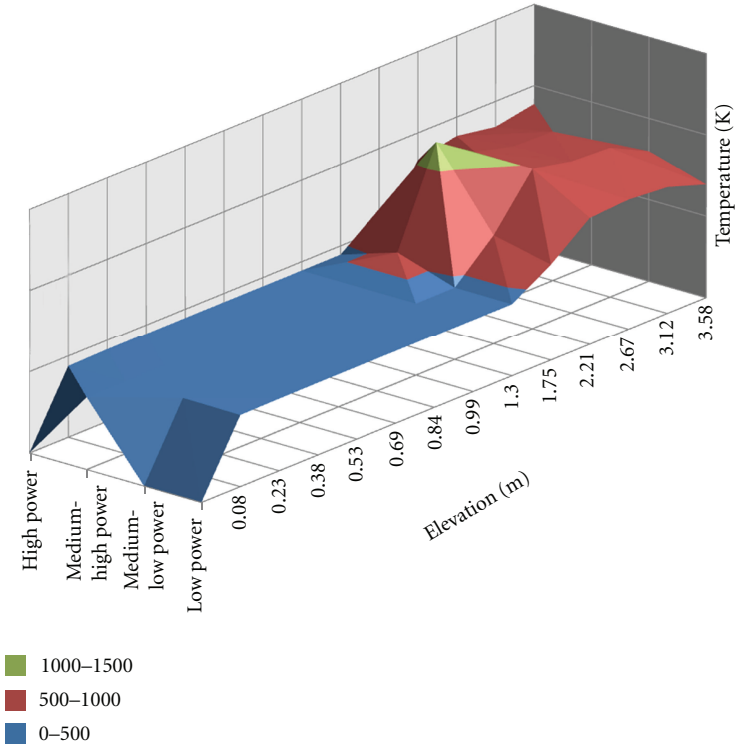

Figure 36: Core temperature distribution at 5.1 hours for scenario with water injection at 4.9 hours after scram (all emergency water injection was terminated at 4.2 hours after reactor scram).

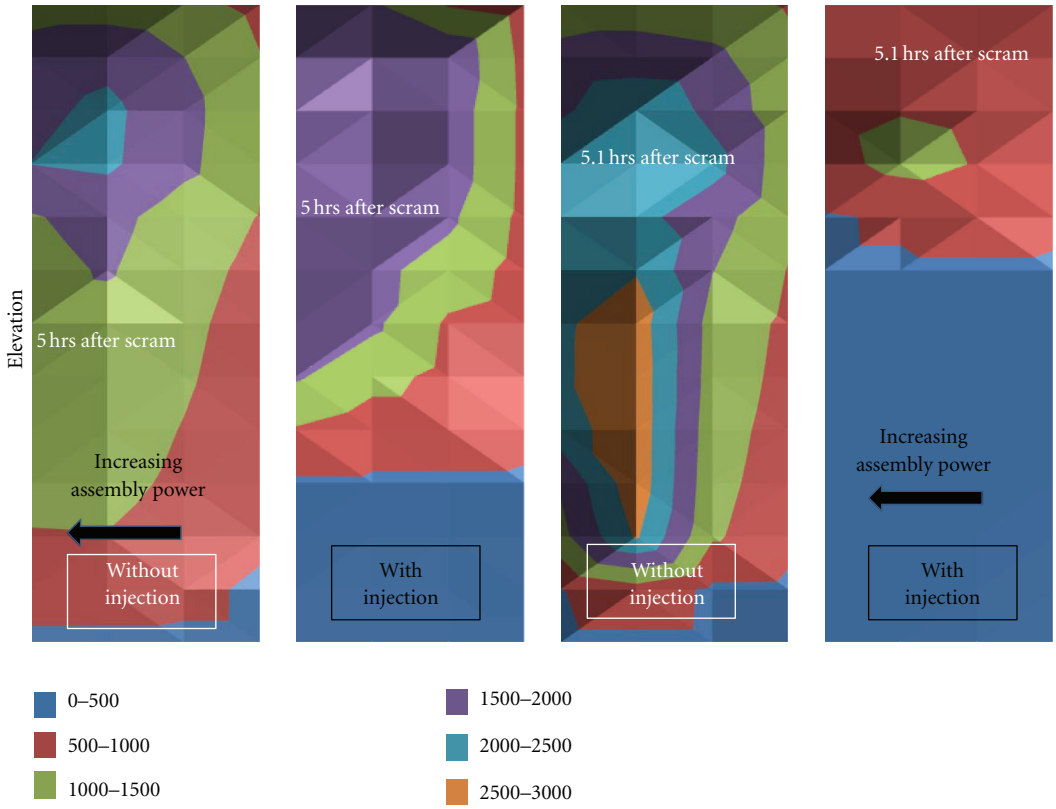

Figure 37: Core temperature distributions for scenarios with depressurization with and without water injection after core uncovery (all emergency water injection was terminated at 4.2 hours after reactor scram).

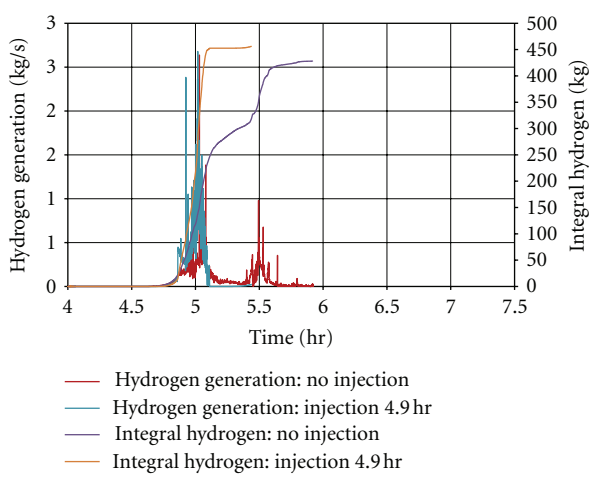

Figure 38: Hydrogen generation rate and integral hydrogen for scenarios without water injection and with water injection at 4.9 hours after scram (all emergency water injection was terminated at 4.2 hours after reactor scram).

What are the general conclusions for severe accident management strategies?

(a) Detailed analysis for realistic bounding scenarios like the station blackout scenario can provide general guidance of timing of important events like core uncovery, loss of control blades, fuel melting, and slumping of molten material into the lower plenum as well as likely consequences such as hydrogen and radionuclide release to the containment.

(1) The likely response of the measureable system parameters including core exit temperatures, pressures, water levels for different accident strategies such as, depressurization, and water addition can be determined on a plant-specific

basis including the influence of uncertainties in models, measurements, and timing of operator actions.

(2) Detailed desktop severe accident simulations for representative plant designs and bounding conditions can be performed in real time to provide guidance to regulatory and other advisory emergency response teams (the RELAP/SCDAPSIM calculations presented in Sections 5 and 6 were performed at 2–5 times faster than real time on a standard Windows laptop computer).

(b) The responses to the accident once the accident is underway can make a significant difference in the consequences of the accident.

(1) Normal emergency procedures that result in termination or limiting of emergency core cooling, that is, the termination of core cooling via the isolation condenser in the case of Fukushima Daiichi Unit 1 and termination of emergency core cooling in the case of TMI-2, need to be reevaluated in light of the potential consequences if instrument readings are faulty or external circumstances change.

(2) Accident management strategies that do not consider, under bounding accident scenarios, the realistic times required for the core (a) to be uncovered and (b) to be damaged (including the failure of control blades and fuel melting) may unnecessarily greatly increase the amount of core/vessel damage without clear benefits in reducing the consequences of the accident. For example, the timing for reactor vessel depressurization once core cooling has been lost or impeded can make a very significant difference in the timing and extent of core damage. Specifically, in a station blackout scenario, premature or early depressurization of the reactor vessel can accelerate the initiation and extent of fuel melting. Delayed depressurization may increase the likelihood of high-pressure vessel ejection and, as demonstrated in the Fukushima Daiichi scenario, can delay or prevent the injection of water into the vessel.

(3) Strategies to inject water into the core should also consider the negative impact of water injection including (a) the accelerated destruction of control blades and other damage to the core (b) and significant increases in the rate, and possibly amount, of hydrogen production.

Acronyms

ISS: Innovative Systems Software
CNSNS: Comision Nacional de Seguridad Nuclear y Salvaguardias
IAEA: International Atomic Energy Agency
SDTP: SCDAP Development and Training Program
KIT: Karlsruhe Institute of Technology
BWR: Boiling water reactor
PWR: Pressurized water reactor
PBF: Power Burst Facility
SDT: Severe Damage Test
ST: Scoping Test
CORA: KIT test facility
Quench: KIT test facility
PHEBUS: Test reactor at Cadarache, France
LOFT: Facility at Idaho National Laboratory
RCS: Reactor coolant system
RPV: Reactor Pressure Vessel
RCIC: Reactor core isolation cooling
CRD: Control rod drive
SRV: Safety relief valve
FP: Fission product
TMI-2: Three Mile Island Unit 2
OECD: Organisation for Economic Co-operation and Development.

References

[1] C. M. Allison and J. K. Hohorst, "SDTP—developing technology for the nuclear industry," in *Proceedings of the 13th International Conference on Nuclear Engineering (ICONE13-50979)*, Beijing, China, May 2005.

[2] http://www.relap.com/.

[3] C. M. Allison and J. K. Hohorst, "Role of RELAP/SCDAPSIM in nuclear safety," *Science and Technology of Nuclear Installations*, vol. 2010, Article ID 425658, 2010.

[4] C. M. Allison, R. J. Wagner, L. J Siefken, and J. K. Hohorst, "The development of RELAP5/SCDAPSIM/MOD4.0 for reactor system analysis and simulation," in *Proceedings of the 7th International Conference on Nuclear Option in Countries with Small and Medium Electricity Grids*, Dubrovnik, Croatia, May 2008.

[5] http://quench.forschung.kit.edu/82.php/.

[6] S. Hagen, P. Hofmann, V. Noack, G. Schanz, G. Schumacher, and L. Sepold, "The CORA-program: out-of-pile experiments on severe fuel damage," in *Proceedings of the 5th International Topic Meeting on Nuclear Thermal Hydraulics, Operations, and Safety*, Beijing, China, April 1997.

[7] D. J. Osetek, "Results of the four PBF severe fuel damage tests," in *Proceedings of the 15th Water Reactor Safety Information Meeting (NUREG/CP-0090)*, Gaithersburg, Md, USA, October 1987.

[8] E. W. Coryell, "Summary of Important Results and SCDAP/RELAP5 Analysis for OECD LOFT Experiment LP-FP-2," Tech. Rep. NUREG/CR/6160, EGG-2721, Nuclear Energy Agency-Committee on the Safety of Nuclear Installations-R, 1994.

[9] RELAP5 Code Development Team, "RELAP5/MOD 3.3 code manual, Vol. 1–8," NUREG/CR-5535/Rev1, December 2001.

[10] SCDAP/RELAP5 Development Team, "SCDAP/RELAP5/MOD3.2 code manual, Vol. 1–5," NUREG/CR-6150, INEL-96/0422, July 1998.

[11] B. Tóth, A. Bieliauskas, G. Bandini et al., "Benchmark study on fuel bundle degradation in the phebus FPT2 test using state-of-the-art severe accident analysis codes," *Nuclear Technology*, vol. 169, no. 2, pp. 81–96, 2010.

[12] C. M. Allison and J. K. Hohorst, "An assessment of RELAP/SCDAPSIM/MOD3.4 using the phebus FPT-2 bundle heating and melting experiment," in *Proceedings of the International Congress on Advances in Nuclear Power Plants (ICAPP '05)*, pp. 3284–3293, American Nuclear Society, Seoul, Republic of Korea, May 2005.

[13] J. H. Spencer et al., "Assessment of new modeling in RELAP/SCDAPSIM using experimental results from the Quench program," in *Proceedings of the International Congress on Advances in Nuclear Power Plants (ICAPP '11)*, Nice, France, May 2011.

[14] C. M. Allison, "Recent improvements in RELAP/SCDAPSIM/MOD3.4 resulting from QUENCH and PARAMETER bundle heating and quenching experiments," in *Proceedings of the 8th International Conference of Nuclear Options in Countries with Small and Medium Electricity Grids*, Dubrovnik, Croatia, 2010.

[15] S. Hagen, P. Hofmann, V. Noack, L. Sepold, G. Schanz, and G. Schumacher, *Large Bundle PWR Test CORA-18: Test Results*, Forschungszentrum Karlsruhe—FZKA-6031, 1998, http://www.cfn.kit.edu/.

[16] P. Hofmann, "Metallographic examination of the severe fuel damage scoping test (SFD-ST) fuel rod bundle cross sections," NUREG/CR-5119, EGG-2537, 1988.

[17] A. Stefanova et al., "SARNET benchmark on QUENCH-11—final report," Forschungszentrum Karlsruhe—FZKA 7368, 2008, http://quench.forschung.kit.edu/82.php.